Global Plasma Turbulence Simulations of $q = 3$ Sawtoothlike Events in the RTP Tokamak

M. R. de Baar,[1] A. Thyagaraja,[2] G. M. D. Hogeweij,[1] P. J. Knight,[2] and E. Min[1]

[1]*FOM Institute for Plasma physics Rijnhuizen,* Association EURATOM-FOM, Trilateral Euregio Cluster, P.O. Box 1207, 3430 BE Nieuwegein, The Netherlands*

[2]*Euratom/UKAEA Fusion Association, Culham Science Centre, Abingdon OX14 3DB, United Kingdom*

(Received 23 September 2004; published 24 January 2005)

A two-fluid computer model of electromagnetic tokamak turbulence, CUTIE, is used to study the dynamic structure and turbulent transport in the Rijnhuizen Tokamak Project tokamak. A discharge with dominant, off-axis electron cyclotron heating is the main focus of the simulations which were extended over several resistive diffusion times. CUTIE reproduces the turbulent transport and MHD phenomena of the experiment. The noninductive components of the current density profile, viz., the dynamo current and the bootstrap current, are identified as key players in the turbulent transport and its suppression and in off-axis MHD events.

DOI: 10.1103/PhysRevLett.94.035002 PACS numbers: 52.25.Fi, 52.55.Fa, 52.50.Gj

The transport of energy, momentum, and particles in tokamaks [1] is not fully understood. The ''anomalous'' component of this is thought to be due to low frequency (i.e., $\omega \ll \Omega_i$, where Ω_i is the ion gyrofrequency) turbulence that could have both electrostatic as well as electromagnetic components. The aim of this Letter is to investigate the dynamics of tokamak turbulence and the extent to which it determines phenomena observed in the Rijnhuizen Tokamak Project (RTP) tokamak [2–4]. We present simulations of electromagnetic, two-fluid tokamak turbulence using the CUTIE code [5,6], and elucidate the key profile-turbulence interactions responsible for a variety of transport and MHD phenomena observed in the experiment. RTP was a small, well diagnosed, tokamak (major radius $R = 0.72$ m, minor radius $a = 0.16$ m), with dominant electron cyclotron heating (ECH). Moving the ECH power deposition radius r_{dep} in steps of 1 mm from the plasma center to half radius showed seven regions in which moving r_{dep} hardly affected the central electron temperature $T_{\mathrm{e}}(0)$ [2]. These regions were separated sharply, as could be appreciated from steplike transitions of $T_{\mathrm{e}}(0)$. The transitions are the consequence of the loss of transport barriers in the electron channel. Off-axis sawtoothlike magnetohydrodynamic (MHD) events [4] imply that the barriers are close to the simple rationals in the safety factor profile $q(r)$, i.e., near the $q = 1$, $4/3$, $3/2$, 2, $5/2$, and 3 surfaces. The profiles of the discharges with the ECH deposition approximately at half radius show steady-state off-axis maxima in $T_{\mathrm{e}}(r)$. Purely diffusive heat fluxes can account for central minima only when there are significant sinks. However, it was concluded that neither the electron-ion energy exchange nor the total radiated power provide such sinks [3]. In this Letter we show that an outward advective heat flux must exist in the core of these discharges.

We focus on the turbulent dynamics of the quasistationary, off-axis sawtoothing phase of an ECH heated discharge. The simulated and experimental conditions have identical macroscopic parameters. The plasma current $I_p = 80$ kA, the toroidal field $B_{\mathrm{tor}} = 2.24$ T, and the line average density $\bar{n}_e \simeq 3 \times 10^{19}$ m^{-3}. The ECH power (350 kW) is deposited at $r_{\mathrm{dep}}/a = 0.55$ with a localization of approximately 1 cm. RTP's aspect ratio, $R_0/a = 4.4$, allows a periodic cylinder ordering. Its small minor radius results in $\rho^* = \rho_s/a \simeq 10^{-2}$, where $\rho_s \equiv C_s/\Omega_i$; $C_s^2 \equiv (T_e + T_i)/m_i$; $\Omega_i = eB_{\mathrm{tor}}/m_i c$, m_i is the ion mass (hydrogen in RTP), and e is the charge. The neoclassical resistive time scale is about 15 ms. These parameters enable a relatively long-time (50 ms) simulation with the following parameters: time step $\Delta t = 25$ ns, 100 radial grid points, 32 poloidal and 16 toroidal harmonics. The equations used to evolve $T_{e,i}$, $n = n_e \simeq n_i$, ion parallel velocity $v_\parallel$, electrostatic potential Φ, and parallel vector potential Ψ are

$$\frac{\partial n}{\partial t} + \nabla \cdot (n\mathbf{v}) = S_p, \tag{1}$$

$$m_i n \frac{d\mathbf{v}}{dt} = -\nabla(p_e + p_i) + \mathbf{j} \times \mathbf{B}/c + \mathbf{F}_{\mathrm{eff}}, \tag{2}$$

$$\frac{3}{2}\left[\frac{dp_{e,i}}{dt}\right] + p_{e,i}\nabla \cdot \mathbf{v}_{e,i} = -\nabla \cdot \mathbf{q}_{e,i} + P_{e,i}, \tag{3}$$

$$\mathbf{E} + \mathbf{v}_e \times \mathbf{B}/c = -\nabla p_e/en + \mathbf{R}_e, \tag{4}$$

where $\mathbf{j} = c\nabla \times \mathbf{B}/4\pi$. Details of the reduced equations are available in [5,6]. We split the total magnetic field, $\mathbf{B} = \nabla\psi \times \hat{\mathbf{e}}_\zeta + B_{\mathrm{tor}}\hat{\mathbf{e}}_\zeta$, where $\hat{\mathbf{e}}_\zeta$ is the unit vector in the ''toroidal'' direction. The electric field is given by $\mathbf{E} = -\frac{1}{c} \times \frac{\partial\psi}{\partial t}\hat{\mathbf{e}}_\zeta - \nabla\phi$. The particle source is represented by S_p, while the effective force on the plasma is taken to be $\mathbf{F}_{\mathrm{eff}} \propto (\nabla \cdot m_i n D_{\mathrm{turb}} \nabla \mathbf{v})$, where D_{turb} is a ''turbulent momentum diffusivity'' (effectively a subgrid, high wave number cutoff [6]) taken proportional to the mean square local vorticity and the current density. The electron-ion friction force is $\mathbf{R}_e$, while $\mathbf{q}_{e,i}$ are the heat-flux vectors. All quan-

tities are split into a flux-surface average (functions of r, t only) and a not necessarily small fluctuating part dependent on r, θ, ζ, t. Mesoscales, time scales between the Alfvén time [$t_A = qR_0/V_A$; $V_A = B_{tor}/(4\pi m_i n_e)^{1/2}$] and the resistive time ($\tau_{res} = 4\pi a^2/c^2\eta_{nc}$), and length scales L_{meso} satisfying $\rho_s < L_{meso} < a$ are modeled. The nonlinear physics of shear Alfvén, drift tearing, and ballooning modes are described by the equations of motion (but not trapped particle or electron temperature gradient-driven fine-scale instabilities). When subject to external sources (in our case a localized ECH power source), the system gives rise to turbulence with regions of mesoscale variations of profiles. A key feature of CUTIE is that these profile corrugations interact nonlinearly with the turbulence which reacts back on the profiles. The induction equation,

$$\frac{\partial\langle B_\theta\rangle}{\partial t} = c\frac{\partial\langle E_\zeta\rangle}{\partial r}, \tag{5}$$

where $\langle\,\rangle$ denotes averaging over a flux surface, and $\langle E_\zeta\rangle = \eta_{nc}(\langle j_\zeta\rangle - j_{bs} - j_{dyn})$; the "dynamo current," $j_{dyn} = \langle\hat{\mathbf{e}}_\zeta \cdot (\delta\mathbf{v}\times\delta\mathbf{B})\rangle/c\eta_{nc}$, exemplifies this feature. Furthermore, η_{nc}, j_{bs} are the neoclassical resistivity and bootstrap current density [1,7], respectively, and $j_\zeta = \frac{c}{4\pi}\frac{1}{r}\frac{\partial rB_\theta}{\partial r}$. The radial electric field $\langle E_r\rangle$ is determined by averaging the radial momentum balance

$$E_r = \hat{\mathbf{e}}_r \cdot \left[-\frac{\mathbf{v}\times\mathbf{B}}{c} + \frac{1}{en}\nabla p_i\right]. \tag{6}$$

Here the poloidal flow velocity (toroidal flows are neglected in this work) satisfies

$$\frac{\partial\langle u_\theta\rangle}{\partial t} = \nu_{nc}(u_{nc} - \langle u_\theta\rangle) + \langle L_\theta\rangle, \tag{7}$$

where ν_{nc} is the flow-damping rate and u_{nc} is the poloidal velocity in neoclassical theory [7]. The poloidal acceleration, $\langle L_\theta\rangle = -\frac{1}{r}\frac{\partial}{\partial r}(r\langle\delta u_\theta \delta u_r\rangle) + \hat{\mathbf{e}}_\theta \cdot \frac{\langle\delta\mathbf{j}\times\delta\mathbf{B}\rangle}{m_i n}$, is the sum of turbulent Reynolds and Maxwell stress contributions. These equations and the particle and energy transport equations of a similar general structure [6] determine the self-consistent evolution of all relevant profiles. The radial heat transfer via the electrons is composed of a (diffusive) Rechester-Rosenbluth term $\langle q_{\|e}\mathbf{b}\cdot\hat{\mathbf{e}}_r\rangle$, and a turbulent advection term $\frac{3}{2}\langle\delta p_e \delta v_r\rangle$. The neoclassical terms are negligible in the electron energy balance. Both the turbulent advection term and the diffusive Rechester-Rosenbluth term are driven by the fluctuating electromagnetic fields. A simple model source, $S_p(r) \propto [1 - 1.2(\frac{r}{a})^2]$, including a sink at the edge ($r/a > 0.9$) is used. A density feedback system injects particles into the plasma whenever $\bar{n}_e < 3\times 10^{19}$ m^{-3}. Given the experimental uncertainties in obtaining a realistic particle source profile, the simulated n_e profiles are not expected to be quantitatively accurate. Our simulations were carried out for approximately three resistive times ($\simeq 50$ ms) starting with an arbitrary initial state with noise levels of turbulence. The code achieves quasistationary, fully developed turbulence with nontrivial dynamic structures in about 25 ms. The initial evolution is itself of interest, but not directly comparable with experiment as the starting state is arbitrary. The q and T_e profiles evolve episodically as the turbulence develops and q crosses certain rational values.

In this Letter we present the results obtained from the 30–50 ms epoch of evolution. Around 30 ms, $T_e(r)$ develops a significant central minimum of about 430 eV and an off-axis maximum of $\simeq 650$ eV, close to r_{dep}. At this time, regular, off-axis "sawtooth" oscillations appear, and both q and T_e relax periodically about their mean values. The details of this dynamic structure, in which transport, turbulence, and current relaxation combine in synergy, are now discussed.

In Fig. 1(a) we show the simulated temporal evolution of $T_e(0)$ and $T_e(r_{dep})$; Fig. 1(b) shows the corresponding q waveforms. The $T_e(r_{dep})$ sawteeth amplitudes are of order 150 eV and have a period of roughly 3.3 ms. The central oscillation is in the order of 100 eV. We see also that q sawtooths between 2.8 and 3 at r_{dep} while $q(0)$ has much larger oscillations between 2.8 and 3.7. The $m = 3, 4$, $n = 1$ MHD modes are the principal ones associated with these phenomena. It is interesting to observe in the temperature waveforms some high frequency "precursors" to the crashes as well as "postcursors." There is evidence of partial crashes, and the waveforms are not strictly periodic. The ramp time is about 3 ms, and the crash time roughly 0.3 ms.

Both initial and time-averaged (30–50 ms) profiles of $T_{e,i}$, q, n_e are shown in Figs. 2(a) and 2(b). It can be seen that a significant evolution of profiles occurs in 30 ms. The time-averaged q profile is mildly inverted with a flat region around $q = 3$. The instantaneous profiles (not shown) reveal a periodically relaxing "elbow" close to the heating radius. Note that while the time-averaged T_e profile is inverted, the T_i profile is not. Neither q nor T_i were diagnosed in the experiment. The time-averaged n_e profile results from the turbulence and the imposed, centrally peaked particle source.

We now explain the sustainment of pronounced off-axis maxima in T_e, found in our simulations, in agreement with

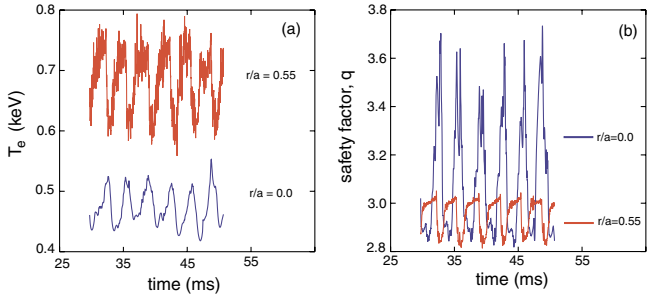

FIG. 1 (color online). (a) Simulated T_e, and (b) q waveforms.

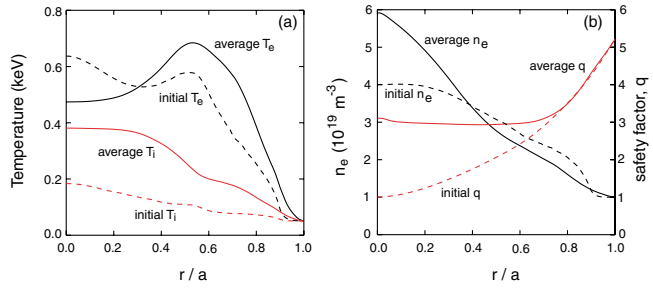

FIG. 2 (color online). Initial and time-averaged profiles: (a) $T_{e,i}$; (b) n_e, q.

experiment. As stated, radiative loss is estimated to be negligible from the core in RTP [3,4] and is not modeled in CUTIE. The electron-ion heat exchange and the central Ohmic heating are relatively small terms in the power balance in the simulations. In Fig. 3(a) we plot the time-averaged power densities of ECH, Ohmic power $\simeq$ 100 kW, and the power into the ions. It follows that an outward (i.e., positive) advective heat flux must exist and be driven up the gradient towards r_{dep} in order to balance the inward heat diffusion. The average advective electron heat-flux component in the core is always positive, as shown in Fig. 3(b), and explains the reason for the calculated inverted T_e profile in Fig. 2(a). This has a minimum near r_{dep} and also explains the ''ear'' or off-axis maximum in T_e. The secondary minimum at $r/a = 0.75$ is related to the weaker barrier at that radius. The flat q profile is due to self-organization of the system due to the combined operation of the turbulent dynamo current and the bootstrap effects. The relaxation process itself is synergistic, involving the self-consistent zonal flows, dynamo currents, and the profile-turbulent interactions with highly corrugated spatial structures.

Figure 4(a) shows the self-consistently calculated, time-averaged poloidal zonal flow (from 30–50 ms) $v_{\mathrm{zonal}} = -cE_r/B$. It is driven by the ion pressure gradients as well as by turbulent Reynolds stresses. Figure 4(b) shows time-averaged total (toroidal) current density profile, j_{tot}, j_{dyn}, and j_{bs} profiles. Both v_{zonal} and j_{dyn} exhibit strongly sheared structures, especially in the neighborhood of the heating radius. They also have rapid variations with time (not shown here). The zonal flow shear can decorrelate the turbulence and also cause enhanced damping [6]. Some of the generation mechanisms relevant to them have recently been discussed [8]. In addition, turbulence is suppressed in CUTIE by low magnetic shear (a consequence of the rather flat total current density profile). The suppression mechanisms via E_r' and q' interact synergistically via j_{bs} and p' (not shown).

We discuss next the effect of the two noninductive components of the current, j_{dyn} and j_{bs}, on the evolution of the system. The dynamo current, j_{dyn}, is driven by turbulent Reynolds stresses and j_{bs} is mainly driven by pressure gradients [7]. Both reduce the magnetic shear. j_{dyn} is larger and more rapidly varying in time and space (''corrugated'') than j_{bs}.

The magnetic modes with larger widths drive the dynamo term j_{dyn}, which reduces the magnetic shear around the modes, increasing their extent. Thus the q profile is clamped at simple rationals. When two low (m, n) modes form within the power deposition radius, a competition for maximum mode size starts and a current ''jet'' is compressed between the two modes. Such current layers form ''elbows'' in the q profile. Finally, the off-axis sawteeth oscillations are caused by periodic relaxations due to the profile-turbulence interaction via j_{dyn}. Switching off j_{dyn} in the induction equation leads to a very different, low amplitude MHD response, although qualitative features of the q profile remain invariant.

The bootstrap current is smaller, but its effect is no less striking in the barrier dynamics: j_{bs} flattens q and changes the driving terms of turbulence. Because of the intense heating, a mode forms in the vicinity of the power deposition radius. Asymmetric fluxes caused by the mode give rise to the formation of a high p' (and j_{bs}) region. The lower m modes imply more radially asymmetric and extended fluxes. The effect occurs in the vicinity of a low rational in the q profile, simultaneously reducing the density of rational surfaces due to lowered magnetic shear [9]. This rapid spatiotemporal shear variation tends to suppress finer-scale modes and saturates the nonlinear MHD modes

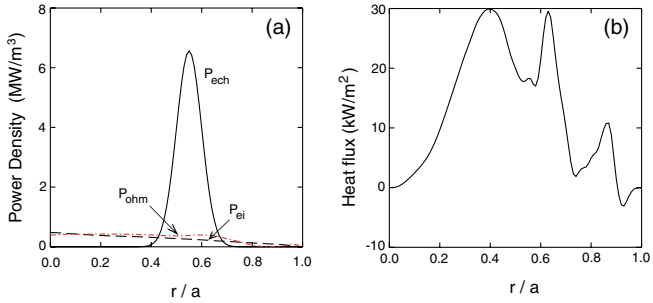

FIG. 3 (color online). Time-averaged (a) P_{ech}, P_{ohm}, P_{ei}, and (b) advective electron heat flux.

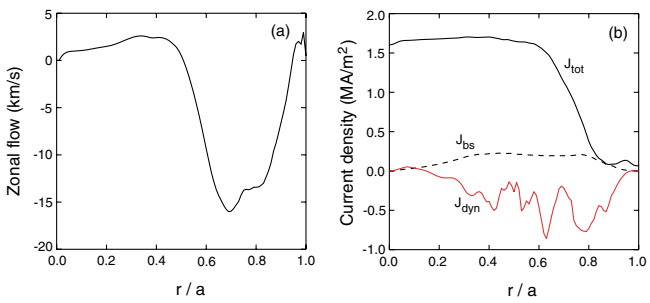

FIG. 4 (color online). Time-averaged (a) zonal flow, and (b) j_{tot}, j_{dyn}, j_{bs}.

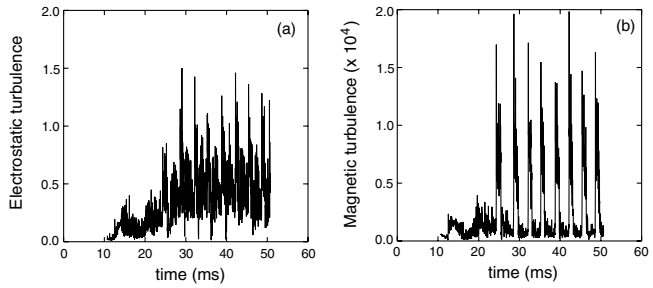

FIG. 5. Waveforms of (a) $\langle(\delta v_r/v_d)^2\rangle$, and (b) $\langle(\delta B_r/B_{\rm pol})^2\rangle$.

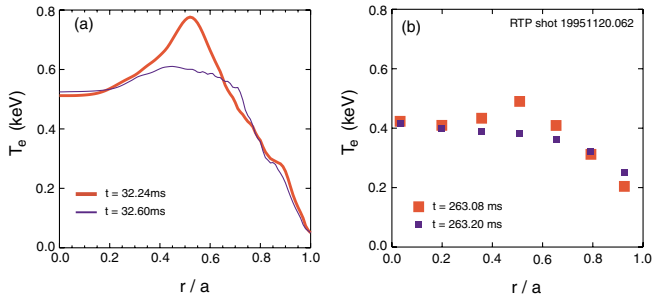

FIG. 6 (color online). (a) Simulated T_e profiles at crash, and (b) experimental T_e profiles at crash.

due to current profile flattening. The barrier and the q profile are thus coupled via $j_{\rm dyn}$, $j_{\rm bs}$, and the resonant modes.

In Figs. 5(a) and 5(b), the waveforms of the volume-averaged intensities of electrostatic turbulence [$\langle(\delta v_r/v_{\rm d})^2\rangle$, the radial velocity perturbation relative to a typical poloidal drift velocity] and magnetic turbulence [$\langle(\delta B_r/B_{\rm pol})^2\rangle$] are presented, including the initial development (from 10 ms). We observe two distinct developed turbulence levels: one associated with the background turbulence, the other with large scale, quasiperiodic MHD events. During MHD events, the diffusive transport (down the temperature gradient) does result in rises of central temperature with a delay, as shown in Fig. 1(a). The background turbulence causes, within the heating radius, a significant outward electron energy transport [cf. Fig. 3(a)]. This sustains the off-axis maximum.

Strong magnetic activity is associated with these sawtoothlike oscillations [Fig. 5(b)]. In addition to the heat flow, current is redistributed outward during the events and $q_{r_{\rm dep}}$ decreases whereas q_0 rises [Fig. 1(b)]. The cause for these events in the simulations is a coupling of an outer (4, 1) mode and an inner (3, 1) viscoresistive tearing mode driven by the dynamo current action. The events involve considerable fine structure. There are compound crashes and rapid temporal variations of zonal flows and dynamo currents, together with avalanching of temperature on both sides of the heating radius down the gradient. This shows that the profile dynamics and the turbulent transport are fundamentally linked. In Figs. 6(a) and 6(b) we show the simulated and experimental (from a discharge with similar, but not exactly identical parameters) T_e profiles just before and after a sawtooth crash. We see that the off-axis maximum is ''chopped off'' by the sawtooth crash, after which the released energy flows towards the core of the plasma and towards the edge. This was also observed in the experiments.

In summary, CUTIE simulations of RTP discharges with dominant off-axis ECH have been carried out. The electromagnetic, quasineutral two-fluid model with the dynamo term, self-consistent zonal flows, and neoclassical effects qualitatively reproduces many salient mesoscale features of the experiment [e.g., $\tau_E \simeq 3$ ms (experiment), 3–4 ms (theory)].

The code positions barriers near rational q radii and naturally generates an outward heat advection for off-axis ECH discharges which is sufficient for supporting off-axis maxima (''ears'') in the T_e profile, comparable to the experimental observations. Both self-generated zonal flows and dynamo currents appear to play an important role. Off-axis sawtooth events (''ear choppers'') are reproduced in the simulations, due to a coupling of an outer (4, 1) mode and an inner (3, 1) viscoresistive tearing mode driven by the dynamo current action. This is believed to be the first time an electromagnetic turbulence-based tokamak transport code evolved on a resistive time scale has been able to reproduce global dynamical structures like off-axis sawteeth as a consequence of profile-turbulence interactions and plasma self-organization.

This work was supported by the European Communities under the contracts of Association between EURATOM/FOM and EURATOM/UKAEA. The views and opinions expressed herein do not necessarily reflect those of the European Commission. It was jointly funded by Euratom, NWO, and the United Kingdom Engineering & Physical Sciences Research Council.

*Electronic address: www.rijnh.nl

[1] J. A. Wesson, *Tokamaks* (Clarendon Press, Oxford, 1997), pp. 12–13.
[2] M. R. de Baar *et al.*, Phys. Rev. Lett. **78**, 4573 (1997).
[3] G. M. D. Hogeweij *et al.*, Phys. Rev. Lett. **76**, 632 (1996).
[4] G. M. D. Hogeweij *et al.*, Nucl. Fusion **38**, 1881 (1998).
[5] A. Thyagaraja, Plasma Phys. Controlled Fusion **42**, B255 (2000).
[6] A. Thyagaraja, P. J. Knight, and N. Loureiro, Eur J. Mech. B/Fluids **23**, 475 (2004).
[7] R. D. Hazeltine and J. D. Meiss, *Plasma Confinement* (Addison-Wesley, New York, 1992).
[8] D. R. McCarthy, C. N. Lashmore-Davies, and A. Thyagaraja, Phys. Rev. Lett. **93**, 065004 (2004).
[9] X. Garbet *et al.*, Phys. Plasmas **8**, 2793 (2001).